Title: Shifts in stability and control effectiveness during evolution of the Avialae support aerial maneuvering hypotheses for flight origins

Authors: D. Evangelista[1*†], S. Cam[1], T. Huynh[1], A. Kwong[2], H. Mehrabani[2], K. Tse[3], R. Dudley[1‡]

Affiliations:

[1]Department of Integrative Biology, University of California, Berkeley CA.

[2]Department of Bioengineering, University of California, Berkeley CA.

[3]Department of Mechanical Engineering, University of California, Berkeley, CA.

[4]Smithsonian Tropical Research Institute, Balboa, Panama.

*Correspondence to: devangel77b@gmail.com.

†Current address: Department of Biology, University of North Carolina at Chapel Hill, NC.

Abstract: The capacity for aerial maneuvering shaped the evolution of flying animals. Here we evaluate consequences of aviaian morphology for aerial performance (*1,2*) by quantifying static stability and control effectiveness of physical models (*3*) for numerous taxa sampled from within the lineage leading to birds (Avialae, *4*). Results of aerodynamic testing are mapped phylogenetically (*5-9*) to examine how maneuvering characteristics correlate with tail shortening, fore- and hindwing elaboration, and other morphological features (*10*). In the evolution of the Avialae we observe shifts from static stability to inherently unstable aerial planforms; control effectiveness also migrated from tails to the forewings. These shifts suggest that some degree of aerodynamic control and and capacity for maneuvering preceded the evolution of strong power stroke. The timing of shifts suggests features normally considered in light of development of a power stroke also play important roles in control.

One Sentence Summary: The dinosaurs that ultimately became birds possessed long, feathered tails and feathers on their legs along with feathers on their forelimbs unlike the tails of living birds; both fore- and hindlimbs along with the tail could serve to control the animal in the air (like the tails on airplanes), and by tracing out how aerodynamic control changed through time, we show how aerial maneuvering was a major factor in avian evolution.

Main Text:

Regardless of how aerial behavior originates, once airborne an organism must control (*2*) its orientation and position in order to safely navigate the vertical environment (i.e. gliding and directed aerial descent, *1*). Such abilities are present even in taxa with no obvious morphological adaptation for flight; at low speeds, such as at the start of a fall or jump, inertial mechanisms allow for rolling, pitching, and yawing; as speeds increase (or as appendages grow in area), aerodynamic mechanisms of control can be employed. Body and appendage configuration position affect both stability, the tendency to resist perturbations, as well as production of torques and forces for maneuvering (control effectiveness). In the four-winged mid-Cretaceous *Microraptor gui*, changes in planform, such as alternative reconstruction postures or removal of leg and tail feathers, alter stability and the control effectiveness of appendages (*3*). Furthermore, appendage function can shift entirely according to the aerial environment (e.g. asymmetric wing

pronation producing yaw at high glide angle versus roll at low glide angle) or even completely reverse function (*3*). Such results are exciting but are based on a single specimen (*11*). Stronger conclusions can be drawn from comparative study of several forms within a phylogenetic context.

One obvious trend in avian evolution is the transition from long tails and feathered legs in early forms (*11–14*) to later (including extant) forms for which the tail has fused into a short pygostyle and asymmetric flight feathers are absent from the legs. Functional consequences of this shift remain speculative (*15–17*). Similarly, changes in the pectoral girdle have been assumed to enhance a powered downstroke (*4,10*), but may also have influenced maneuvering by shifting the center of body mass (*18*) or in enabling the production of wing asymmetries.

To examine these patterns and to cross-test adaptive hypotheses (*19*), we can use model tests to quantify the effect of shape on stability and control effectiveness3, using specimens sampled from early avialan (*4*) evolution (*6–8*). We hypothesize that within the Avialae, the presence or absence of stability in the various axes and the control effectiveness of the appendages should correlate with changes in major morphological features (shortening of the tail, enlargement of the forewings) to enhance aerodynamic performance. Alternatively, both stability and control may have been absent early in the evolution of flight, only appearing after a strong and bilaterally symmetric power stroke evolved.

Representative aerodynamic measurements for pitching stability and control effectiveness are given in Fig. 1 for seven avialans. Tables and plots of all aerodynamic measurements are provided in the Supplemental Information. Long-tailed taxa (Fig. 1.a) show a stable equilibrium point and the tail is effective in generating pitching moments, whereas short-tailed taxa (Fig. 1.b) were unstable and had reduced control effectiveness of the tail. Notably, the same pattern (i.e., downward sloping C_m versus α) is seen consistently in two early representatives of the Avialaes, in a long-tailed pterosaur (*Rhamphorynchus*), and in the mid-Cretaceous dromaeosaur *Microraptor*, suggesting that these patterns more likely derive from shape and aerodynamics than from immediate ancestry.

All aerodynamic measurements were coded into both discretized and continuous character matrices (see Supplemental Information), which were then mapped onto the phylogeny to examine the evolution of static stability and control effectiveness.

The Avialae show progressive tail loss as well as loss of leg-associated control surfaces along with a concomitant increase in forewing size and bony features associated with the pectoral girdle (nodes 1-4 on Fig. 2). Changes in stability and control effectiveness reflect these morphological changes. In pitch (Fig. 2), taxa shift from being statically stable ancestrally to subsequently being unstable (and thus requiring active control). Control effectiveness concomitantly migrates from the ancestrally large and feathered tail and legs to the increasingly capable forewings, which become relatively larger, gain larger muscle attachments and gain skeletal features that improve production of fine left-right and fore-aft kinematic asymmetries needed for control.

Transition to forewing control correlates with elongation of the coracoid, along with other changes in the scapula (Fig. 2, node 2); in addition, the sternum becomes modified (although a strong keel has not yet developed) (*10*). Concomitantly, the tail becomes much reduced into a pygostyle (Fig. 2, node 3). Other synapomorphies (Fig. 2, node 4) appear in the mid-Cretaceous,

including the strut-like coracoid, triosseal canal, synsacrum and carinate sternum. Whereas the latter features (node 4) feature in power production, the timing of the former features (nodes 2 and 3) appears consistent with enhanced forewing control effectiveness. Ontogenetic tests (*20*) show 4-day post hatching Chukar Partridge are capable of extreme maneuvers (rolling and pitching 180°) before strong development of a carinate sternum, suggesting this interpretation is correct.

In roll (Fig. 3), taxa were stable at high angles of attack, but either unstable or marginally stable at low angles of attack; large asymmetric wing movements (i.e., wing tucking) was always effective in creating substantial rolling moments.

In yaw, all taxa at high angles of attack (Fig. 4a) were marginally stable as might be expected from symmetry. Taxa with long tails were also stable at low angle-of-attack (Fig. 4b) but as tails are reduced, yaw stability is lost and control must again migrate to the wings. Asymmetric wing pronation and supination (Fig. 4a and 4b) was effective in generating yawing moments in all taxa, suggesting maneuverability in yaw early in bird evolution. As the tail becomes shorter, flight becomes marginally stable or unstable, and control effectiveness must migrate (as in pitch control) from the shortening tail to the enlarging forewings. Stability in roll and in yaw shifts with angle of attack, which may serve as a proxy for glide angle or the steepness of descent. At high angles of attack, roll is the more stable axis, whereas stability in yaw is greater at low angles of attack. Forewing asymmetrical movements were effective in all taxa, whereas forewing symmetrical movements were only effective in later taxa.

The findings suggest that the capacity for maneuvering characterized the early stages of flight evolution (*1*), before forewings with a power stroke fully evolved. The large tail of early Avialaes yielded high aerodynamic control effectiveness and the body possessed some degree of stability. Combined with likely dynamic forces and torques generated by either tail whipping (*21*) or reduced amounts of asymmetric or symmetric forewing flapping, this suggests that the ancestral organisms were very capable of controlled aerial behaviors at high angles of attack (Figs. 2-4). Subsequent shifts in control would be consistent with more shallow glides facilitated by incipient wing flapping, which may have served initially in control but then ultimately became the power stroke characteristic of modern birds. Incipient flapping may thus have become elaborated as a control response (*2*) to instabilities demonstrated here. Active control was required as static stability was reduced and eventually lost, and associated forewing movements would also have enhanced aerodynamic force production and provided a means for inertial attitude adjustment. Once the transition to wing-mediated maneuverability and control began, larger surfaces and increased musculature would have facilitated dynamic force production for weight offset via the power stroke characteristic of modern birds.

Materials and Methods. We constructed models (8 cm snout-vent length) of four extant birds, six avialans (*4*) plus *Microraptor* (*11*) and *Anchiornis* (*12*) as outgroups, using 3D printing (*22*) (Supplementary Figs. S1 and S2). Fossils were selected to sample available phylogenies. To explore parallel evolution and for calibration, we also constructed models of three pterosaurs, two bats, and two artificial test objects (sphere and weather vane). Theropods were reconstructed with wings spread and legs extended back (*3,23*) (Supplementary Figs. S2 and S3). For control effectiveness, we tested appendage movements previously identified as being aerodynamically effective (*3,20*): asymmetric wing pronation and supination, wing tucking, symmetric wing protraction and retraction, and dorsoventral and lateral movements of the tail (Supplementary

Fig. S3).

Wind tunnel testing used established methods (*3*), with a six-axis sensor (Nano17, ATI, Apex, NC) mounted to a 0.5 inch (12.7 mm) damped sting exiting the model downwind at the center of mass (Supplementary Fig. S2). Testing at 6 ms^{-1} resulted in a Reynolds number of ~32,000 for all models, matching full scale for Archaeopteryx. Under these conditions the aerodynamic coefficients of interest are reasonably constant with Re (*3,20*).

Sensor readings were recorded at 1000 Hz using a data acquisition card (National Instruments, Austin, TX) (*3*). The sting was mounted to a servo (Hitec USA, Poway, CA) interfaced to a data acquisition computer, using an Arduino microcontroller (SparkFun, Boulder, CO) and specially written code in Python and R (*24*), to automate positioning and measurement of windspeed and force/torque. We then computed non-dimensional force and moment coefficients, static stability coefficients, and control effectiveness (*3,25*). Using the automatic sting, we obtained 13,792 measurements for 247 positions (86 in pitch, 69 in roll, and 92 in yaw).

A Nexus file without branch lengths was assembled from published phylogenies (*6–9*) of the study taxa. Mapping of discrete maneuvering traits was performed in Mesquite (*5*) with the built-in ancestral state reconstruction routines using unordered parsimony. Aerodynamic measurements were coded into a matrix giving eight discretized stability values (stable, marginal, unstable); ten discrete morphological traits, and 12 discretized control effectiveness values (using a threshold of 0.09, chosen based on the weather vane measurements). Additional information is provided in the Supplementary materials.

References and Notes:

1. R. Dudley, S. Yanoviak, Animal aloft: the origins of aerial behavior and flight. *Integr. Comp. Biol.* **51**, 926-936 (2011).
2. J. M. Smith, The importance of the nervous system in the evolution of animal flight. *Evolution* **6**, 127-129 (1952).
3. D. Evangelista *et al.*, Aerodynamic characteristics of a feathered dinosaur measured using physical models . Effects of form on static stability and control effectiveness. *PLoS ONE* (2014).
4. J. Gauthier, K. Padian, in *Beginnings of the Birds: Proceedings of the International* Archaeopteryx *Conference,* M. Hecht, J. Ostrom, G. Viohl, P. Wellnhover, Eds. (Freunde des Jura-Museums, 1985) pp. 185–197.
5. W. P. Maddison, D. R. Maddison, *Mesquite: A modular system for evolutionary analysis.* (2010). http://mesquiteproject.org
6. ZH. Zhou, FZZ. Li, A new Lower Cretaceous bird from China and tooth reduction in early avian evolution. *Proc. R. Soc. B.* **277**, 219-227 (2010).
7. Q. Li *et al.*, Plumage color patterns of an extinct dinosaur. *Science* **327**, 1369-1372 (2010).
8. J. O'Connor, L. M. Chiappe, A. Bell, in *Living Dinosaur: Evolutionary History of the Modern Birds,* G. Dyke, G. Kaiser, Eds. (John Wiley & Sons, 2011) pp. 39–105.

9. J. Cracraft *et al.*, in *Assembling the Tree of Life,* J. Cracraft, M. J. Donoghue, Eds. (Oxford University Press, 2004) pp. 468–489.

10. M. J. Benton, *Vertebrate Paleontology* (Blackwell Publishing, 2005).

11. X. Xu *et al.,* Four-winged dinosaurs from China. *Nature* **421**, 335-340 (2003).

12. D. Hu, L. Hou, L. Zhang, X. Xu, A pre-*Archaeopteryx* troodontid theropod from China with long feathers on the metatarsus. *Nature* **461**, 640–643 (2009).

13. N. Longrich. Structure and function of hindlimb feathers in *Archaeopteryx lithographica*. *Paleobiology* **32**, 417–431 (2006).

14. P. Christiansen, N. Bonde, Body plumage in *Archaeopteryx*: a review, and new evidence from the Berlin specimen. *Comptes Rendus Palevol* **3**, 99–118 (2004).

15. J. M. Smith, Birds as aeroplanes. *New Biol.* **14**, 64–81 (1953).

16. C. W. Beebe, A tetrapteryx stage in the ancestry of birds. *Zoologica* **2**, 39–52 (1915).

17. A. Thomas, On the tails of birds. *Bioscience* **47**, 215–225 (1997).

18. V. Allen, K. T. Bates, Z. Li, J. R. Hutchinson, Linking the evolution of body shape and locomotor biomechanics in bird-line archosaurs. *Nature* **497**, 104–107 (2013).

19. K. Padian, Cross-testing adaptive hypotheses: Phylogenetic analysis and the origin of bird flight. *Amer. Zool.* **41**, 598–607 (2001).

20. D. Evangelista, thesis, University of California, Berkeley (2013).

21. A. Jusufi, D. Goldman, S. Revzen, R. Full, Active tails enhance arboreal acrobatics in geckos. *Proc Nat Acad Sci USA* **105**, 4215–4219 (2008).

22. J. Munk, thesis, University of California, Berkeley (2011).

23. X. Xu, ZH. Zhou, FC. Zhang, XL. Wang, KW. Kuang, Functional hind-wings conform to the hip structure in dromaeosaurids. *J. Vert. Palaeo.* **24**:251 (2004).

24. R Core Team. R: A Language and Environment for Statistical Computing. (2013). http://www.r-project.org/

25. B. W. McCormick, *Aerodynamics, Aeronautics and Flight Mechanics.* (John Wiley and Sons, 1995).

26. ZH. Zhou, FC. Zhang, A long-tailed seed-eating bird from the Early Cretaceous of China. *Nature* **418**, 405-409 (2002).

27. ZH. Zhou, FC. Zhang, *Jeholornis* compared to *Archaeopteryx*, with a new understanding of the earliest avian evolution. *Naturwissenschaften* **90**, 220-225 (2003).

28. CL. Gao *et al.*, A new basal lineage of early Cretaceous birds from China and its implications on the evolution of the avian tail. *Palaeontology* **51**, 775-791 (2008).

29. ZH. Zhou, FC. Zhang, Anatomy of the primitive bird *Sapeornis chaoyangensis* from the early Cretaceous of Liaoning, China. *Can J. Earth Sci.* **40**, 731-747 (2003).

30. LH. Hou, ZH. Zhou, L. Martin, A. Feduccia, A beaked bird from the Jurassic of China.

Nature **377**, 616-618 (1995).

Acknowledgments: We thank Y. Munk, Y. Zeng, E. Kim, M. Wolf, N. Sapir, V. Ortega, S. Werning, K. Peterson, J. McGuire and R. Fearing for their advice and assistance. We than the Berkeley Undergraduate Research Apprentice Program (URAP) and the help of G. Cardona, C. Chun, M. Cohen, E. Guenther-Gleason, V. Howard, S. Jaini, F. Linn, C. Lopez, A. Lowenstein, D. Manohara, D. Marks, N. Ray, A. Tisbe, F. Wong, O. Yu and R. Zhu. DE was supported by an NSF Minority Graduate Research Fellowship, UC Chancellor's Fellowship, and NSF Integrative Graduate Education and Research Traineeship (IGERT) #DGE-0903711. TH was supported by the University of California Museum of Palaeontology (UCMP). We also thank T. Libby and the Berkeley Center for Integrative Biomechanics in Education and Research (CIBER) for use of a force sensor and 3D printer.

Author Contributions: DE wrote the main manuscript text with assistance from RD and TH; DE and TH prepared figures; all authors contributed to the manuscript. The authors declare that they have no competing financial interests.

Fig. 1. Representative aerodynamic measurements for pitching stability and control effectiveness. Long-tailed taxa (A) have a stable equilibrium point at 10-25° (yellow line) and the tail is effective in generating pitching moments at low angles-of attack (pale yellow box). In short-tailed taxa (B), the equilibrium point at 0-5° is unstable (red line) and the tail control effectiveness is reduced. One example (*Rhamphorynchus*) drawn from pterosaurs illustrates similar possibilities in a phylogenetically distant taxon.

Fig. 2. Evolution of pitch stability and control effectiveness within the Avialae. Pitching stability is plotted in red hues, indicating stable (pale), marginally stable (medium), and unstable (solid). Control effectiveness of the tail in generating pitching moments is plotted in orange hues, indicating large control effectiveness (pale) or reduced control effectiveness (solid). Control effectiveness of symmetric wing protraction/retraction is plotted in yellow hues indicating large (pale) or reduced (solid). Consilience among the three traits indicates that early in the evolution of the Avialae, taxa are stable with a large degree of pitch control from the tail; later taxa are unstable, and control has migrated from the now reduced tail, to the wings, which become larger and develop skeletal features that would enhance control and the production of left-right and fore-aft asymmetries.

Fig. 3. Evolution of roll stability and control effectiveness in the Avialaes. Characters shown are stability at low angle of attack (mostly unstable due to symmetry; *Zhongornis* and *Sapeornis* marginal); stability at high angles of attack (all stable); and control effectiveness of asymmetric wing tucking in roll (always effective). As animals developed the ability to fly at reduced body angles of attack, more active control of roll would have been necessary, at first perhaps using inertial modes of the tail, but subsequently augmented with the forewings.

Fig. 4. Evolution of yaw stability and control effectiveness in the Avialaes. At high angles of attack (A), taxa are mostly marginally stable as might be expected from symmetry. Asymmetric pronation and supination of the wings are always effective in generating yaw at high angles of attack. At reduced angles of attack (B), by contrast, long-tailed taxa are stable and can control yaw with the tail. As tails reduce in size, taxa become unstable in yaw at low angles of attack and lose the ability to control yaw with the tail. However, asymmetric movements of the wings are effective in producing yaw throughout the evolution of this clade, and control would thus have shifted from the tail to the forewings paralleling the shifts seen in pitch.

Supplementary Materials:

Physical model details. We tested physical models (~8 cm snout-vent length) of four extant birds and eight theropods, as well as three pterosaurs, two bats, and two artificial shapes (sphere and weather vane). The source fossils are listed in Table S4 and shown in Fig. S1. 3D solid models (Figs. S2A, S2B, Table S5) were developed using Blender (The Blender Foundation, Amsterdam, the Netherlands), closely referencing published photographs of impression fossils and reconstructions from the literature to match long bone, axial skeletal, and body proportions. The models were then printed using a 3D printer (ProJet HD3000, 3D Systems, Rock Hill, SC). Models were mounted on steel armatures and finished with felt, polymer clay, surgical tape, and paper using established methods (*3*).

Aerodynamic testing details. Wind tunnel tests used established methods (*3*) to test models at

Reynolds number corresponding to full-scale *Archaeopteryx*; checks for scale effects in previous studies of *Microraptor* revealed that the aerodynamic coefficients were insensitive to Re (*3*). Methods were also previously benchmarked to check that the construction techniques adequately modeled feathered surfaces, and that measurements were sufficient to model quasi-static maneuvers observed in extant birds, lizards, and human skydivers.

Static stability was measured by examining the sign of the slope $dC_m/d\alpha$ (positive slope is unstable, negative stable, zero marginally stable, see extended Figs. S2C and S2D) of the non-dimensional pitching moment coefficient near fixed points as the body was subjected to small deflections $d\alpha$ (*3,25*):

$$\text{pitching moment} = M = 0.5\ C_m\ \rho\ U^2\ \lambda$$

Control effectiveness ($dC_m/d\delta$) was measured by deflecting appendages (Fig. S3) by a small amount $d\delta$ and examining the change in pitching moment coefficient. A first-order estimate of maneuvering is obtained from considering the two together and a biomechanical trade-off is apparent: a stable object can resist perturbations from the environment with minimal control effort but will also have difficulty in changing direction (which might be necessary to accomplish aerial righting, navigate in cluttered forests, seek resources or avoid predators). The metrics underestimate maneuvering in very dynamic cases (high advance ratio flapping), but are adequate for quasi-static maneuvers. Locomotion is a complex task, and passive stability is often exploited where possible to reduce control effort; conversely, passive instability may be exploited in extreme (and likely elective) maneuvers. The absence of stability, coupled with the presence of large control effectiveness, could be used to infer the presence of strong closed-loop neuromuscular control. The absence of control effectiveness suggests a lack of control, as even with feedback an ineffective surface cannot generate the necessary forces and torques. Thus, while the full control abilities of an extinct form are difficult if not impossible to fully enumerate, the simple metrics here provide a useful proxy.

Fig. S1. Fossils used for comparative study. Outgroups (A) *Anchiornis* (*12*) and (B) *Microraptor* (*11*); Fossil Avialans (C) *Archaeopteryx* (*10,13*), (D) *Jeholornis* (*26,27*), (E) *Zhongornis* (*28*), (F) *Sapeornis* (*29*), (G) *Zhongjianiornis* (*6*) and (H) *Confuciusornis* (*28,30*); (I) extant birds *Alectoris*, *Columba*, *Larus*, and *Buteo*.

Fig. S2. Model construction, testing, and measurement of static stability and control effectiveness. Models were developed in Blender (A) from fossils (*Archaeopteryx* shown) and constructed and tested (B) using established methods (*3*). For simple cases such as a sphere or a weather vane, the relationship between slope and stability (C) is observed by plotting pitching moments versus angle-of-attack. Nondimensionalized moment coefficients are used to diagnose/examine stability and control effectiveness of the various taxa (D).

Fig. S3. Appendage movements tested to determine control effectiveness. Appendage movements were selected based on those observed to be effective in previous work (*3*), including (A) symmetric wing protraction (e.g. wing sweep); (B) tail dorsiflexion; (C) tucking of one wing; (D) tail lateral flexion; and (E) asymmetric wing pronation/supination.

Table S1. Static stability and control effectiveness in pitch. (A) Pitch stability coefficients are shown as mean ± s.d., n=15. (B) Control effectiveness in pitch using tail dorsiflexion (Fig. S3B), shown as mean ± s.d., n=5. (C) Control effectiveness in pitch using symmetric wing protraction (wing sweep) (Fig. S3A), shown as mean ± s.d., n=5. Colors indicate characters

depicted in Fig. 2.

Table S2. Static stability and control effectiveness in roll. (A) Roll stability coefficients are shown as mean ± s.d., *n*=15. (B) Control effectiveness in roll using asymmetric wing tucking (Fig. S3C), shown as mean ± s.d., *n*=5

Table S3. Static stability and control effectiveness in yaw. (A) Yaw stability coefficients are shown as mean ± s.d., *n*=15. (B) Control effectiveness in yaw using tail lateral flexion (Fig S3D), shown as mean ± s.d., *n*=5. (C) Control effectiveness in yaw using symmetric wing pronation (Fig. S3E), shown as mean ± s.d., *n*=5. (d) Control effectiveness in yaw using head lateral flexion for pterosaurs only, shown as mean ± s.d., *n*=5.

Table S4. Fossil Avialae sampled for aerodynamic testing and references used during model construction.

Table S5. Geometry data for physical models of eight extinct theropod dinosaurs, four extant birds, two bats, three pterosaurs and two objects for checking calibration.

Nexus File S1. A Nexus file without branch lengths was assembled from published phylogenies (*6–9*) of the study taxa. Aerodynamic measurements were coded into a matrix giving eight discretized stability values (stable, marginal, unstable); ten discrete morphological traits, and 12 discretized control effectiveness values (using a threshold of 0.09, chosen based on the weather vane measurements). Corresponding continuous traits are also included.

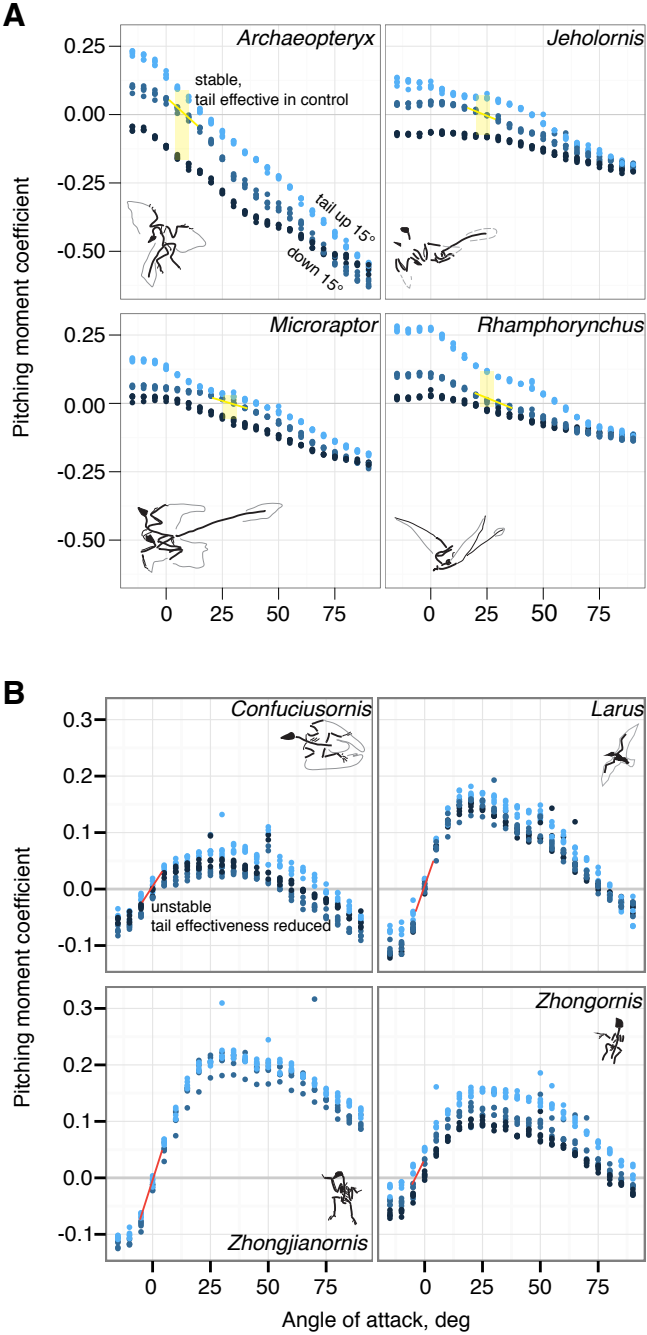
A
Archaeopteryx
Jeholornis
Microraptor
Rhamphorynchus
stable,
tail effective in control
tail up 15°
down 15°
Pitching moment coefficient
0.25
0.00
-0.25
-0.50
0
25
50
75
B
Confuciusornis
Larus
Zhongornis
Zhongjianornis
unstable
tail effectiveness reduced
0.3
0.2
0.1
0.0
-0.1
Angle of attack, deg

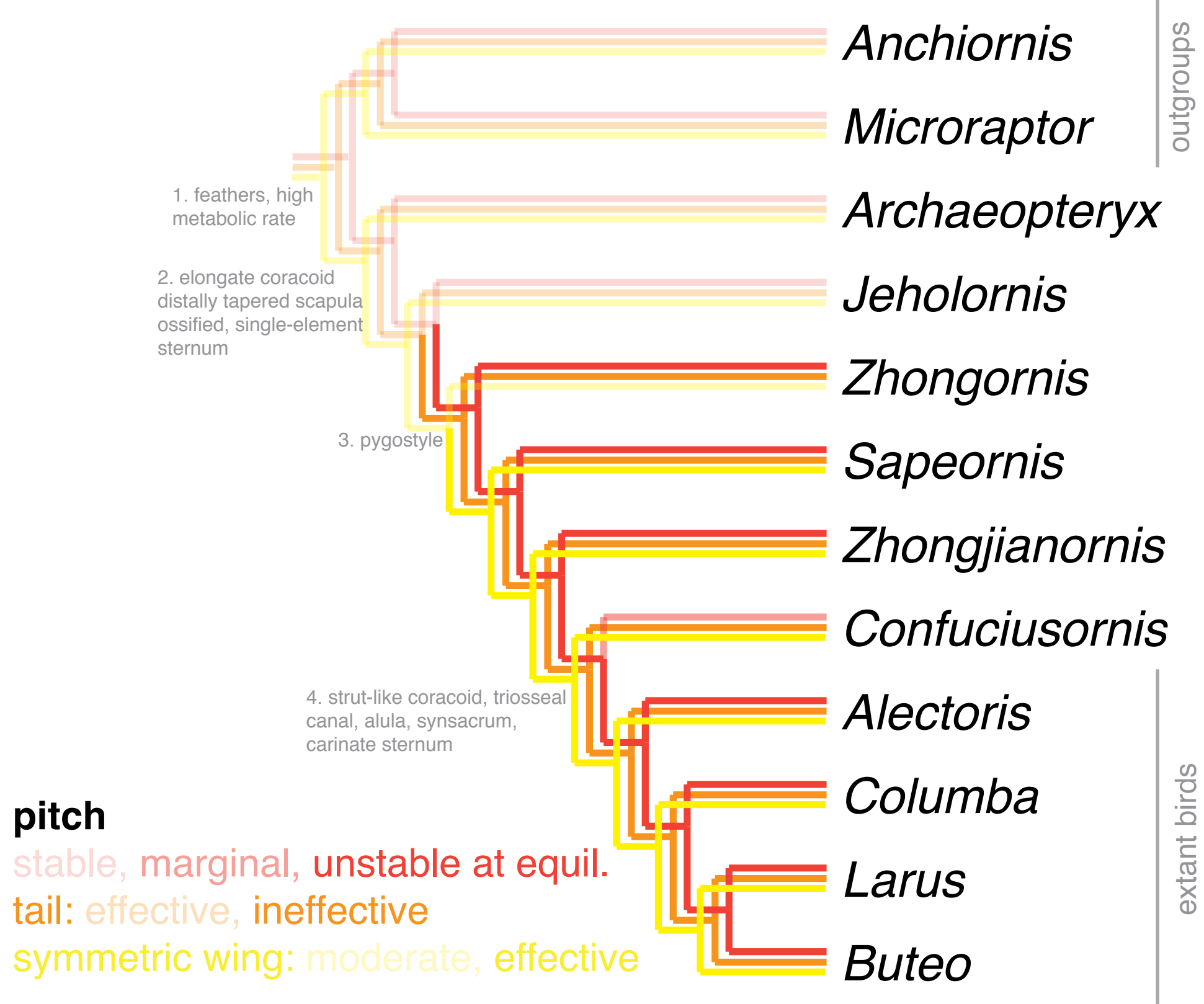
Anchiornis
Microraptor
Archaeopteryx
Jeholornis
Zhongornis
Sapeornis
Zhongjianornis
Confuciusornis
Alectoris
Columba
Larus
Buteo
outgroups
extant birds
1. feathers, high metabolic rate
2. elongate coracoid distally tapered scapula ossified, single-element sternum
3. pygostyle
4. strut-like coracoid, triosseal canal, alula, synsacrum, carinate sternum
pitch
stable, marginal, unstable at equil.
tail: effective, ineffective
symmetric wing: moderate, effective

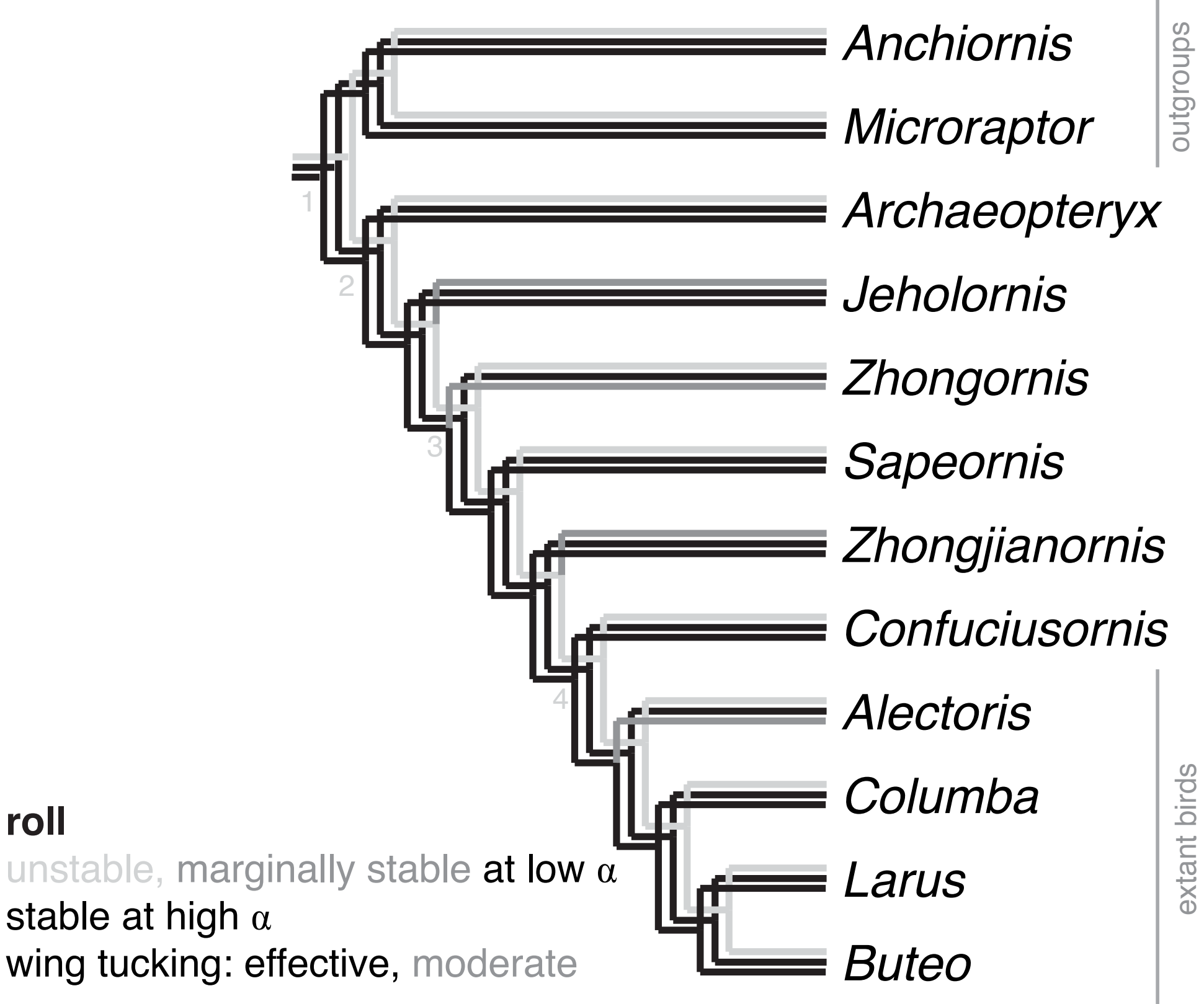
Anchiornis
Microraptor
Archaeopteryx
Jeholornis
Zhongornis
Sapeornis
Zhongjianornis
Confuciusornis
Alectoris
Columba
Larus
Buteo
outgroups
extant birds
1
2
3
4
roll
unstable, marginally stable at low α
stable at high α
wing tucking: effective, moderate

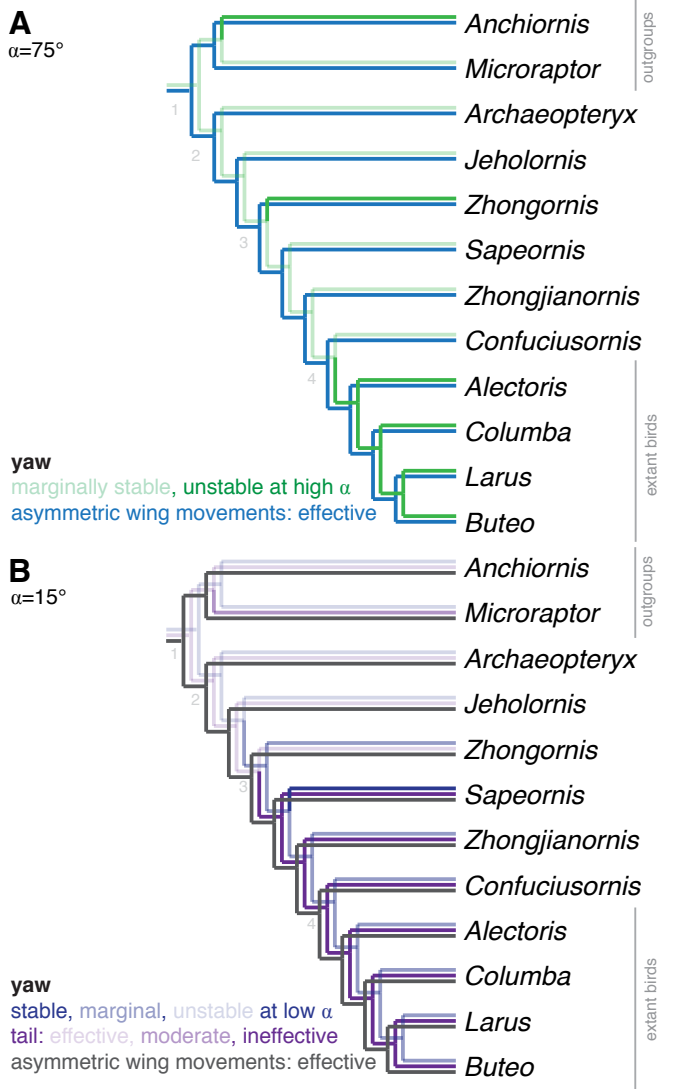
A
α=75°
Anchiornis
Microraptor
Archaeopteryx
Jeholornis
Zhongornis
Sapeornis
Zhongjianornis
Confuciusornis
Alectoris
Columba
Larus
Buteo
outgroups
extant birds
1
2
3
4
yaw
marginally stable, unstable at high α
asymmetric wing movements: effective
B
α=15°
Anchiornis
Microraptor
Archaeopteryx
Jeholornis
Zhongornis
Sapeornis
Zhongjianornis
Confuciusornis
Alectoris
Columba
Larus
Buteo
outgroups
extant birds
1
2
3
4
yaw
stable, marginal, unstable at low α
tail: effective, moderate, ineffective
asymmetric wing movements: effective

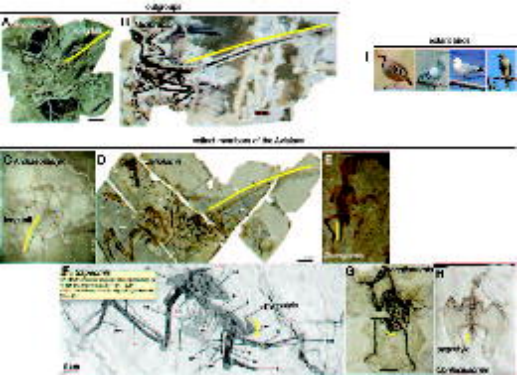

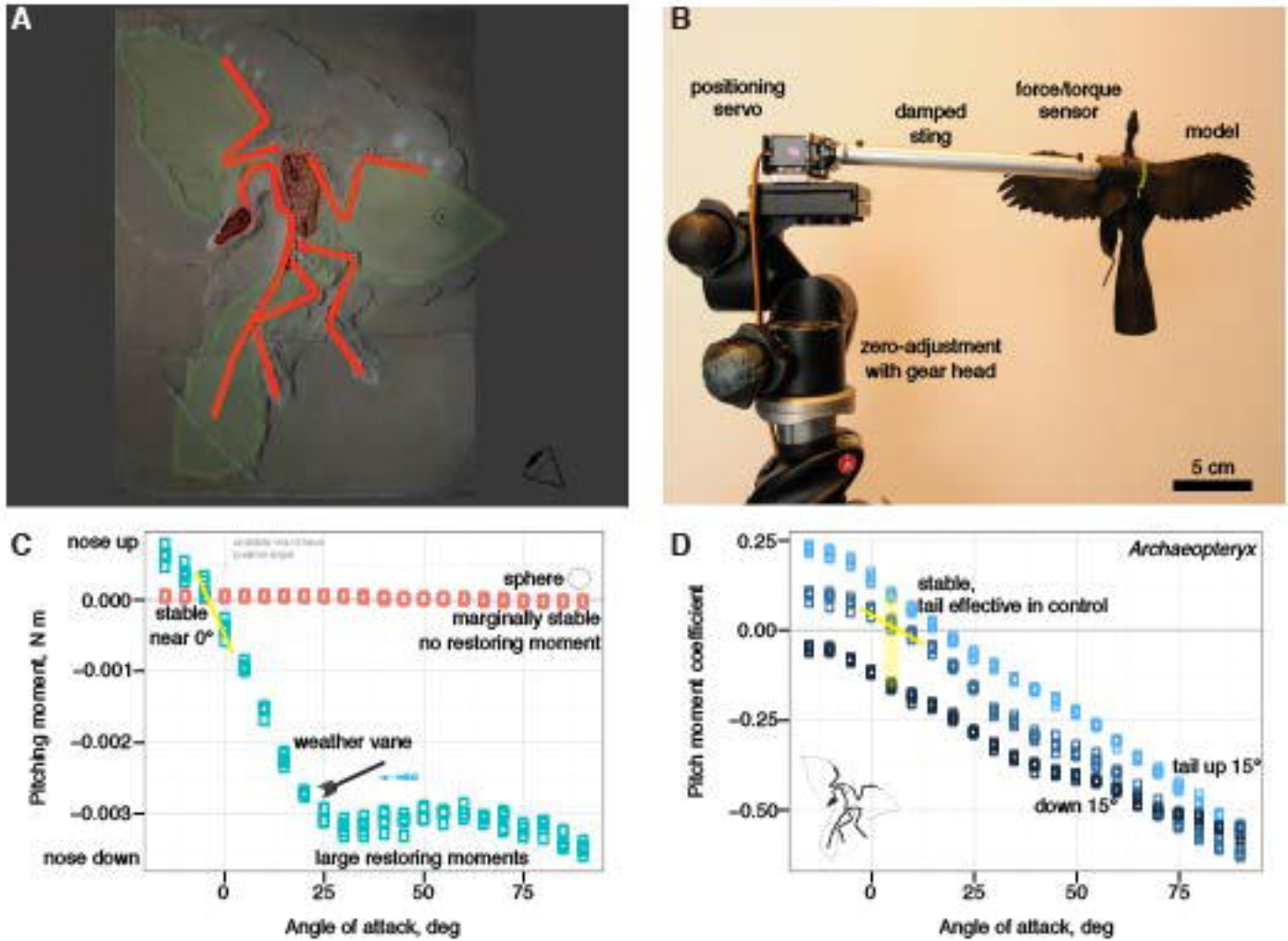
A
B
positioning servo
damped sting
force/torque sensor
model
zero-adjustment with gear head
5 cm
C
nose up
nose down
Pitching moment, N m
0.000
−0.001
−0.002
−0.003
sphere
stable near 0°
marginally stable
no restoring moment
weather vane
large restoring moments
0
25
50
75
Angle of attack, deg
D
Archaeopteryx
Pitch moment coefficient
0.25
0.00
−0.25
−0.50
stable, tail effective in control
tail up 15°
down 15°
0
25
50
75
Angle of attack, deg

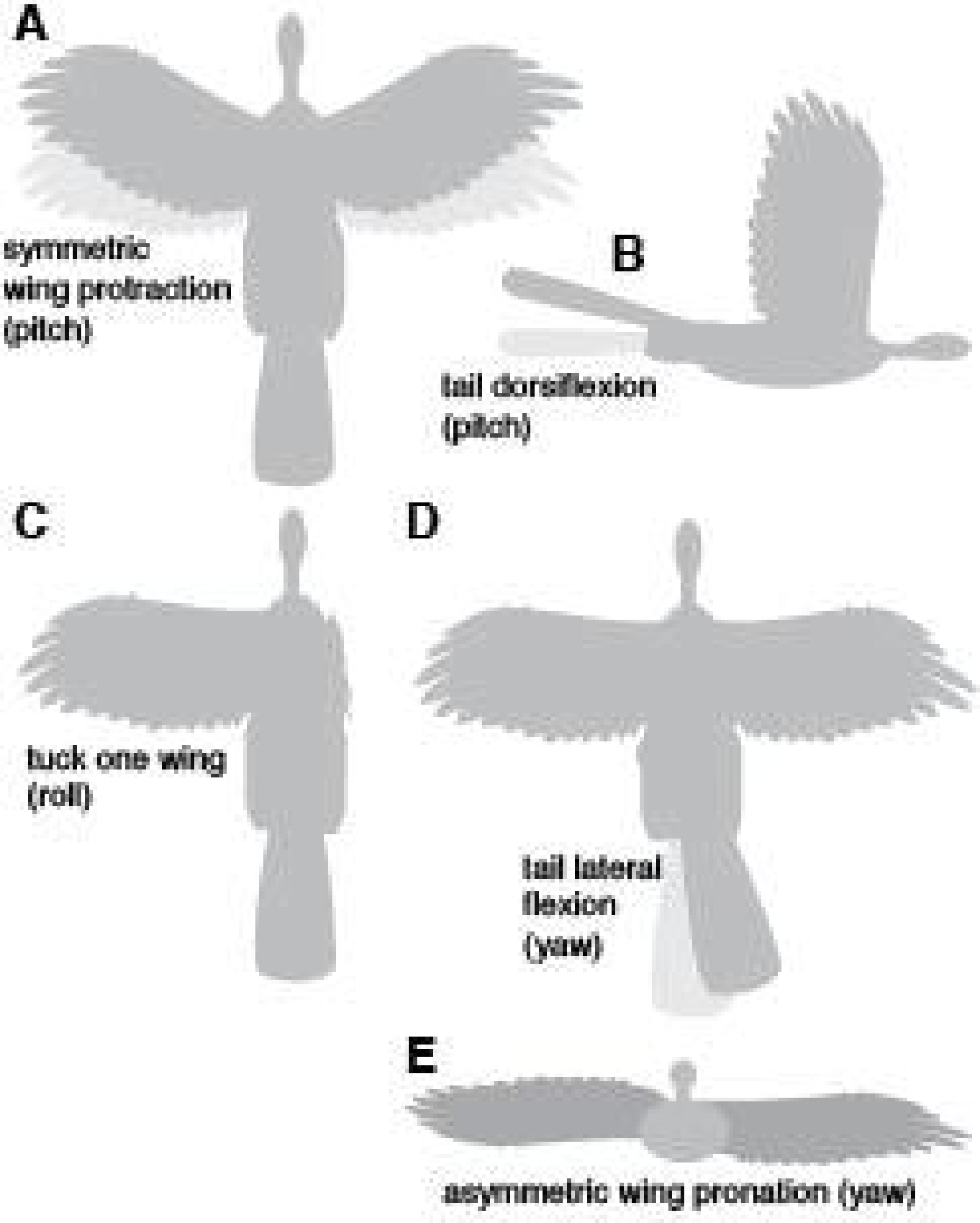
A
symmetric
wing protraction
(pitch)
B
tail dorsiflexion
(pitch)
C
tuck one wing
(roll)
D
tail lateral
flexion
(yaw)
E
asymmetric wing pronation (yaw)

A

	pitch stability, $dC_m/d\alpha$			equilibrium point	
	α=0°	α=15°	α=75°	α°	equilibrium $dC_m/d\alpha$
Anchiornis	-0.005±0.013	-0.067±0.012	-0.13±0.03	29±2	**-0.170±0.028**
Archaeopteryx	-0.134±0.013	-0.221±0.020	-0.18±0.03	9±2	**-0.190±0.012**
Confuciusornis	0.142±0.009	0.039±0.020	-0.06±0.02	0±2	**-0.030±0.073**
Jeholornis	0.011±0.018	-0.108 ±0.010	-0.10±0.02	25±1	**-0.120±0.044**
Microraptor	-0.039±0.006	-0.071±0.009	-0.17±0.02	20±2	**-0.070±0.029**
Sapeornis	0.109±0.010	0.007±0.011	-0.11±0.02	5±2	**-0.100±0.052**
Zhongjianornis	0.305±0.036	0.195±0.027	-0.15±0.16	5±1	**0.180±0.078**
Zhongornis	0.237±0.021	0.084±0.017	-0.11±0.09	0±2	**0.060±0.089**
Alectoris	0.206±0.006	0.090±0.020	-0.37±0.16	0±1	**0.120±0.013**
Buteo	0.187±0.010	-0.042±0.009	-0.13±0.02	0±3	**-0.140±0.030**
Columba	0.046±0.014	-0.047±0.017	-0.18±0.16	0±6	**-0.050±0.088**
Larus	0.352±0.028	0.092±0.015	-0.10±0.02	0±1	**0.150±0.049**
Onychonycteris	-0.011±0.011	-0.112±0.005	-0.12±0.02	10±2	-0.110±0.033
Pteropus	-0.118±0.014	-0.055±0.008	-0.10±0.02	0±2	-0.080±0.015
Pteranodon	0.054±0.023	0.004±0.018	-0.07±0.04	5±3	-0.050±0.029
Pterodactylus	-0.020±0.020	-0.050±0.009	-0.05±0.03	0±4	-0.040±0.009
Rhamphorynchus	-0.062±0.013	-0.192±0.024	-0.05±0.01	15±1	-0.180±0.044
Sphere	-0.037±0.023	-0.020±0.022	-0.03±0.01		-0.050±0.006
Weather vane	-0.333±0.040	-0.347±0.020	-0.03±0.04	0±2	-0.210±0.055

B

	control effectiveness, $dC_m/d\delta$ for tail dorsiflexion*		
	α=0°	α=15°	α=75°
Anchiornis	0.168±0.002	**0.191±0.006**	0.0467±0.0120
Archaeopteryx	0.219±0.007	**0.190±0.010**	0.0649±0.240
Confuciusornis	0.011±0.003	**0.013±0.003**	0.0178±0.0050
Jeholornis	0.268±0.019	**0.223±0.001**	0.0678±0.0050
Microraptor	0.174±0.023	**0.125±0.002**	0.0891±0.0140
Sapeornis	0.054±0.001	**0.064±0.005**	0.0817±0.0060
Zhongjianornis	0.023±0.004	**0.019±0.004**	0.0124±0.0260
Zhongornis	0.049±0.006	**0.048±0.002**	0.0455±0.0030
Alectoris	0.011±0.004	**0.012±0.005**	0.0443±0.0070
Buteo	0.018±0.003	**0.033±0.012**	0.0491±0.0060
Columba	0.044±0.004	**0.050±0.003**	0.0085±0.0020
Larus	0.014±0.008	**0.016±0.003**	0.0137±0.0080
Onychonycteris	0.029±0.004	0.032±0.002	0.004±0.004
Pteropus	0.053±0.009	0.026±0.003	0.026±0.002
Pteranodon	0.016±0.005	0.015±0.002	0.0158±0.0030
Pterodactylus	0.015±0.002	0.025±0.004	0.0388±0.0050
Rhamphorynchus	0.347±0.016	0.245±0.032	0.0288±0.0100

C

	control effectiveness, $dC_m/d\delta$ for symmetric wing protraction†		
	α=0°	α=15°	α=75°
Anchiornis	0.00±0.02	**0.050±0.020**	0.070±0.004
Archaeopteryx	-0.00253±0.016	**0.060±0.018**	0.128±0.0036
Confuciusornis	0.00640±0.034	**0.117±0.023**	0.229±0.0015
Jeholornis	0.04239±0.009	**0.072±0.006**	0.088±0.002
Microraptor	0.01784±0.008	**0.037±0.003**	0.051±0.0036
Sapeornis	0.02174±0.038	**0.173±0.039**	0.329±0.001
Zhongjianornis	0.02522±0.027	**0.119±0.023**	0.221±0.0006
Zhongornis	0.02976±0.012	**0.069±0.010**	0.100±0.0006
Alectoris	-0.00095±0.017	**0.124±0.020**	0.119±0.0017
Buteo	0.04297±0.034	**0.142±0.021**	0.213±0.0013
Columba	0.07612±0.027	**0.151±0.013**	0.168±0.0002
Larus	-0.00706±0.030	**0.110±0.032**	0.231±0.0012
Onychonycteris	0.03101±0.030	0.152±0.031	0.235±0.0025
Pteropus	-0.00490±0.041	0.131±0.030	0.230±0.0023
Pteranodon	0.16728±0.050	0.315±0.033	0.480±0.0014
Pterodactylus	0.00492±0.026	0.088±0.018	0.141±0.0023
Rhamphorynchus	0.01197±0.025	0.045±0.020	0.175±0.0007

* movement depicted in Extended Figure 7b
† movement depicted in Extended Figure 7a

A	roll stability, $dC_m/d\phi$		B	control effectiveness, $dC_m/d\delta$ for asymmetric wing tucking*	
	α=15°	α=75°		α=15°	α=75°
Anchiornis					
Archaeopteryx	0.009±0.060	-0.200±0.019		0.090±0.005	0.200±0.018
Confuciusornis	-0.020±0.020	-0.200±0.09		0.050±0.002	0.100±0.012
Jeholornis	0.073±0.030	-0.400±0.025		0.080±0.004	0.120±0.024
Microraptor	0.132±0.030	-0.300±0.019		0.050±0.007	0.170±0.021
Sapeornis	0.043±0.040	-0.300±0.026		0.080±0.002	0.130±0.016
Zhongjianornis	0.030±0.020	-0.200±0.012		0.050±0.001	0.140±0.015
Zhongornis	0.017±0.040	-0.100±0.080		0.030±0.001	0.050±0.007
Alectoris	0.009±0.060	-0.100±0.016		0.060±0.002	0.080±0.007
Buteo	0.028±0.050	-0.400±0.022		0.170±0.012	0.240±0.055
Columba	-0.030±0.050	-0.300±0.014		0.180±0.007	0.180±0.027
Larus	-0.009±0.020	-0.400±0.028		0.150±0.004	0.200±0.038
Onychonycteris		-1.000±0.044		0.810±0.036	0.880±0.100
Pteropus	-0.027±0.050	-0.700±0.064		0.680±0.020	0.830±0.088
Pteranodon	0.011±0.020	-0.200±0.014		0.070±0.002	0.100±0.010
Pterodactylus	-0.002±0.060	-0.300±0.016		0.100±0.003	0.110±0.027
Rhamphorynchus	-0.0969±0.030	-0.400±0.021		0.160±0.007	0.210±0.030
Sphere	0 (exact)	0 (exact)			

* movement depicted in Extended Figure 7c

A

	yaw stability, $dC_m/d\psi$	
	α=15°	α=75°
Anchiornis	**-0.097±0.003**	**0.006±0.006**
Archaeopteryx	**-0.070±0.004**	**0.010±0.004**
Confuciusornis	**-0.026±0.002**	**0.004±0.002**
Jeholornis	**-0.091±0.003**	**0.002±0.001**
Microraptor	**-0.100±0.016**	**0.039±0.010**
Sapeornis	**0.002±0.003**	**0.005±0.0004**
Zhongjianornis	**0.021±0.003**	**0.008±0.002**
Zhongornis	**0.014±0.002**	**0.00±0.81**
Alectoris	**0.022±0.001**	**0.001±0.002**
Buteo	**0.027±0.006**	**-0.002±0.004**
Columba	**0.048±0.002**	**0.003±0.002**
Larus	**0.017±0.004**	**0.002±0.002**
Onychonycteris	0.025±0.008	-0.040±0.007
Pteropus	0.040±0.025	-0.160±0.005
Pteranodon	0.026±0.002	0.002±0.0004
Pterodactylus	-0.002±0.001	0.002±0.001
Rhamphorynchus	-0.052±0.004	-0.034±0.004

B

	control effectiveness, $dC_m/d\delta$ for lateral tail flexion*	
	α=15°	α=75°
Anchiornis	**0.240±0.070**	0.067±0.013
Archaeopteryx	**0.220±0.070**	0.066±0.004
Confuciusornis	**0.002±0.001**	-0.004±0.001
Jeholornis		-0.027±0.007
Microraptor	**0.520±0.083**	-0.076±0.010
Sapeornis		
Zhongjianornis	**-0.001±0.002**	-0.007±0.001
Zhongornis	**0.007±0.002**	-0.011±0.001
Alectoris	**0.019±0.012**	-0.050±0.001
Buteo	**-0.007±0.003**	-0.029±0.003
Columba	**0.005±0.002**	-0.022±0.001
Larus		-0.012±0.002
Onychonycteris	-0.011±0.005	-0.012±0.003
Pteropus (no tail)		
Pteranodon (no tail)		
Pterodactylus (no tail)		
Rhamphorynchus	0.170±0.008	0.128±0.002

C

	control effectiveness, $dC_m/d\delta$ for asymmetric wing supination†	
	α=15°	α=75°
Anchiornis	**0.199±0.020**	**0.330±0.004**
Archaeopteryx	**0.420±0.015**	**0.383±0.016**
Confuciusornis	**0.206±0.025**	**0.184±0.007**
Jeholornis		
Microraptor	**0.259±0.013**	**0.373±0.008**
Sapeornis		
Zhongjianornis	**0.296±0.015**	**0.262±0.015**
Zhongornis	**0.115±0.006**	**0.113±0.002**
Alectoris	**0.081±0.013**	**0.093±0.004**
Buteo	**0.565±0.060**	**0.431±0.025**
Columba	**0.455±0.042**	**0.204±0.003**
Larus		
Onychonycteris	0.870±0.093	0.627±0.049
Pteropus (no tail)		
Pteranodon (no tail)	0.271±0.013	0.234±0.004
Pterodactylus (no tail)	0.196±0.014	0.139±0.013
Rhamphorynchus	0.279±0.027	0.319±0.024

D

	control effectiveness, $dC_m/d\delta$ for lateral head flexion*	
	α=15°	α=75°
Pteranodon	0.120±0.002	-0.003±0.0005
Pterodactylus	0.190±0.003	0.002±0.001
Rhamphorynchus	-0.033±0.009	

* movement depicted in Extended Figure 7d
† movement depicted in Extended Figure 7e

	specimen and reference	Total length (10^{-2} m)	remarks
Anchiornis	LPM B00169[12]	34	
Microraptor	IVPP V13352[11]	85	
Archaeopteryx	Berlin[10,13]	40	
Jeholornis	IVPP V13274[26,27]	65	Feathers only in 13553
Zhongornis	D2455-2456[28]	10	Weak feather impressions
Sapeornis	IVPP V13275[29]	27	
Zhongjianornis	IVPP V15900[6]	22	
Confuciusornis	Multiple[28,30]	30	

	area (10^{-4} m^2)	snout-vent length (10^{-2} m)	total length (10^{-2} m)	span (10^{-2} m)	aspect ratio
Anchiornis	87.11	7.1	18.0	19.6	2.2
Archaeopteryx	94.57	8.0	10.5	17.7	1.7
Confuciusornis	50.53	6.8	9.2	19.9	3.9
Jeholornis	77.03	7.7	19.0	22.7	3.4
Microraptor	114.6	9.3	22.5	19.2	1.6
Sapeornis	54.44	6.6	7.6	20.7	3.9
Zhongjianornis	61.87	8.3	10.1	21.3	3.7
Zhongornis	44.73	7.7	11.5	15.4	2.7
Alectoris	57.89	7.1	9.8	15.0	2.0
Buteo	98.55	8.3	9.9	23.8	2.9
Columba	80.71	7.3	9.8	19.3	2.3
Larus	72.62	7.9	10.5	24.0	4.0
Onychonycteris	194.7	9.6	13.4	29.5	2.2
Pteropus	201.2	8.4	12.4	35.1	3.1
Pteranodon	42.13	6.4	6.5	22.1	5.8
Pterodactylus	51.15	8.4	8.9	19.0	3.5
Rhamphorynchus	78.56	8.0	18.4	29.7	5.6
Sphere	11.34		3.8	3.8	0.6
Weathervane	39.30		24.0	5.0	0.3